



## Research article

# Resolvin D2-induced reparative dentin and pulp stem cells after pulpotomy in a rat model

Mitsuhiro Yoneda<sup>a</sup>, Hidetaka Ideguchi<sup>b</sup>, Shin Nakamura<sup>c</sup>, Zulema Arias<sup>b</sup>, Mitsuaki Ono<sup>d</sup>, Kazuhiro Omori<sup>b</sup>, Tadashi Yamamoto<sup>e</sup>, Shogo Takashiba<sup>b,\*</sup>

<sup>a</sup> Department of Periodontics and Endodontics, Division of Dentistry, Okayama University Hospital, Japan

<sup>b</sup> Department of Pathophysiology-Periodontal Science, Faculty of Medicine, Dentistry and Pharmaceutical Sciences, Okayama University, Japan

<sup>c</sup> Department of Oral Science and Translational Research, College of Dental Medicine, Nova Southeastern University, USA

<sup>d</sup> Department of Molecular Biology and Biochemistry, Faculty of Medicine, Dentistry and Pharmaceutical Sciences, Okayama University, Japan

<sup>e</sup> The Center for Graduate Medical Education (Dental Division), Okayama University Hospital, Japan

## ARTICLE INFO

## Keywords:

Dental pulp  
Regeneration  
Pulp-capping agents  
Specialized pro-resolving mediators  
Resolvin D2  
Calcification  
Cytokine  
TRPA1  
Animal model

## ABSTRACT

**Introduction:** Vital pulp therapy (VPT) is performed to preserve dental pulp. However, the biocompatibility of the existing materials is of concern. Therefore, novel materials that can induce pulp healing without adverse effects need to be developed. Resolvin D2 (RvD2), one of specialized pro-resolving mediators, can resolve inflammation and promote the healing of periapical lesions. Therefore, RvD2 may be suitable for use in VPT. In the present study, we evaluated the efficacy of RvD2 against VPT using *in vivo* and *in vitro* models.

**Methods:** First molars of eight-week-old male Sprague–Dawley rats were used for pulpotomy. They were then divided into three treatment groups: RvD2, phosphate-buffered saline, and calcium hydroxide groups. Treatment results were assessed using radiological, histological, and immunohistochemical (GPR18, TNF- $\alpha$ , Ki67, VEGF, TGF- $\beta$ , CD44, CD90, and TRPA1) analyses. Dental pulp-derived cells were treated with RvD2 *in vitro* and analyzed using cell-proliferation and cell-migration assays, real-time PCR (*Gpr18*, *Tnf- $\alpha$* , *Il-1 $\beta$* , *Tgf- $\beta$* , *Vegf*, *Nanog*, and *Trpa1*), ELISA (VEGF and TGF- $\beta$ ), immunocytochemistry (TRPA1), and flow cytometry (dental pulp stem cells: DPSCs).

**Results:** The formation of calcified tissue in the pulp was observed in the RvD2 and calcium hydroxide groups. RvD2 inhibited inflammation in dental pulp cells. RvD2 promoted cell proliferation and migration and the expression of TGF- $\beta$  and VEGF *in vitro* and *in vivo*. RvD2 increased the number of DPSCs. In addition, RvD2 suppressed TRPA1 expression as a pain receptor.

**Conclusion:** RvD2 induced the formation of reparative dentin, anti-inflammatory effects, and decreased pain, along with the proliferation of DPSCs via the expression of VEGF and TGF- $\beta$ , on the pulp surface in pulpotomy models.

## 1. Introduction

Dental pulpotomy has been used as a conservative therapy for the pulp exposed to dental caries or trauma. Pulp tissue vitality is crucial for maintaining tooth survival and physiological pulp tissue function [1]; moreover, preserving pulp has reduced the

\* Corresponding author. Department of Pathophysiology - Periodontal Science, Faculty of Medicine, Dentistry and Pharmaceutical Sciences, Okayama University 2-5-1 Shikata-cho, Kita-ku, Okayama, 700-8525, Japan.

E-mail address: [stakashi@okayama-u.ac.jp](mailto:stakashi@okayama-u.ac.jp) (S. Takashiba).

<https://doi.org/10.1016/j.heliyon.2024.e34206>

Received 20 January 2024; Received in revised form 12 June 2024; Accepted 4 July 2024

Available online 6 July 2024

2405-8440/© 2024 The Authors. Published by Elsevier Ltd. This is an open access article under the CC BY-NC-ND license (<http://creativecommons.org/licenses/by-nc-nd/4.0/>).

requirement for treatment, along with improving its cost-effectiveness [2]. Therefore, vital pulp therapy (VPT), using pulp-protective materials with the potential to induce calcification of tissues, has been the focus of research [3]. Calcium hydroxide has long been used as the gold standard [4,5]. Currently, mineral trioxide aggregate (MTA) is replacing calcium hydroxide preparations as the optimal material based on clinical findings [6,7].

VPT promotes immune and inflammatory responses in the dental pulp [8]. As inflammation resolves, cell proliferation is promoted, and the number of endothelial progenitor cells and dental pulp stem cells (DPSCs) increase. Simultaneously, blood vessel maturation and tissue remodeling regenerate the pulp tissue. DPSCs differentiate into odontoblast-like cells to form reparative dentin, thereby protecting the pulp [9]. When chronic inflammation occurs, the appropriate pathway to resolve inflammation by blood cells accumulating in the lesion is disrupted, leading to a failure of tissue regeneration [10]. VPT agents, such as calcium hydroxide and MTA, stimulate pulpal cells, thereby promoting hard tissue formation [9,11]. However, the use of calcium hydroxide and MTA exposes the pulp to a strongly alkaline environment and induces a robust inflammatory reaction that impedes complete and efficient healing [11]. Our overall research objective is to find a biological host modifier that can replace inorganic materials such as calcium hydroxide and MTA as a beneficial therapeutic agent for vital pulp therapy.

Specialized pro-resolving mediators (SPMs), such as omega-3 polyunsaturated fatty acids, have potent pro-resolution effects [12–14]. In rheumatoid arthritis, various SPMs in the synovial fluid that suppress inflammatory symptoms have been identified [15, 16]. In a mouse sepsis model, resolvin D2 (RvD2) reduced mortality by enhancing bacterial clearance without causing immunosuppression [17]. Although anti-inflammatory drugs such as steroids are highly effective in controlling autoimmune diseases, they may cause opportunistic infections. In contrast, SPMs are immunosuppressive and can combat infections [13]. Another type of resolvin (Resolvin E1: RvE1) has been reported to resolve inflammation and to reduce infection, finally induced stem cell-related dentin repairment [18–21]. On the other hand, RvD2 inhibits alveolar bone resorption and exerts anti-inflammatory effects in a mouse periodontitis model [22]. In addition, RvD2 suppresses the progression of apical periodontitis and promotes hard tissue formation in a rat model [23]. These results indicate that RvD2 may also be an ideal reagent for treating various oral diseases, including inflammation and infection.

In the present study, we hypothesized that RvD2 has anti-inflammatory and hard tissue-forming effects in VPT, and that a different mechanism from existing VPT agents might lead to a better consequence. We investigated the effects of RvD2 on dental pulp tissue *in vivo* using a rat pulpotomy model and *in vitro* immunohistochemically using rat dental pulp cells (DPCs).

## 2. Material and methods

The manuscript was prepared according to the Preferred Reporting Items for Laboratory Studies in Endodontology (PRILE) 2021 guidelines [24] and the Preferred Reporting Items for Animal Studies in Endodontology (PRIASE) 2021 guidelines [25] to describe the main stages of the study (Supplemental Figure).

### 2.1. Experimental animals

We used 51 Sprague–Dawley rats (eight-week-old males) for the analysis after excluding samples with death and temporary seal dehiscence (approved by the Animal Care and Use Committee, Okayama University: OKU-2019575, OKU-2022375, OKU-2022679). The present study was conducted following the Animal Research: Reporting of In Vivo Experiments (ARRIVE) guidelines 2.0 [26]. We randomized sequentially the group selection for the control and treatment groups; however, at least three rats were secured in each group.

### 2.2. Pulpotomy model

The pulpotomy model was established as previously described [27]. Under general anesthesia, the coronal pulp tissues of the upper first molars were removed using a #1/4 round bur with a low-speed handpiece. After hemostasis with 5 % sodium hypochlorite, a pledget soaked in 3  $\mu$ L of either RvD2 solution (1  $\mu$ g/mL or 10  $\mu$ g/mL; Cayman Chemical, Ann Arbor, MI, USA) or phosphate-buffered saline (PBS) as negative control was applied to the root canal orifice. Calcium hydroxide paste (Ca(OH)<sub>2</sub>, LIFÉ; Kerr Corporation, Brea,

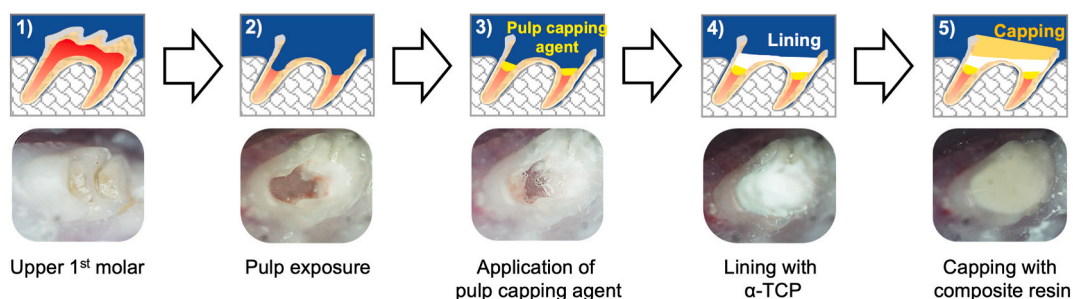


Fig. 1. Representation of the rat pulpotomy experimental protocol.

CA, USA) was applied directly to the root canal orifice using an applicator. Three groups were set as negative control (PBS), positive control (calcium hydroxide), and experimental group (RvD2). The teeth were pre-covered with tricalcium phosphate cement (New Apatite Liner: Dentsply Sirona, Tokyo, Japan) to prevent moisture from the wet pledget, and covered with a light-curing composite resin (Clearfil Majesty; Kuraray Noritake Dental, Tokyo, Japan) to resist mastication force (Fig. 1). The concentration of RvD2 and the sealing method are based on our previous study [23]. After 4 and 6 weeks, rats were euthanized using CO<sub>2</sub>, and their maxillae were removed and fixed in 4 % paraformaldehyde.

### 2.3. Micro-computed tomography (micro-CT) analysis

The fixed maxillae were scanned using a micro-CT scanner and Nrecon system (Skyscan1174 compact micro-CT: Bruker, Kontich, Belgium). The data obtained were analyzed using OsiriX MD (version 12.5; Pixmeo, Geneva, Switzerland). Calcification formed at the treatment site in a slice of the buccolingual surface, including the root canal orifice, and the apex was defined as the reparative dentin. For each sample, three slices were measured every 100 μm. Each root canal area was considered 100 % and compared to the reparative dentin area.

### 2.4. Histological analysis

After the micro-CT analysis, the maxillae were decalcified with 10 % formic acid and embedded in paraffin. Four-micrometer serial sections were prepared for hematoxylin and eosin (H-E) staining or immunohistochemistry. All sections were observed using a DP70 BX-50 light microscope (Olympus, Tokyo, Japan).

### 2.5. Immunohistochemistry (IHC)

Serial sections were stained with primary antibodies raised against the following: G protein-coupled receptor 18 (GPR18; Abcam, Cambridge, England, UK) as the receptor of RvD2 [28], tumor necrosis factor-α (TNF-α; Funakoshi, Tokyo, Japan) as the inflammatory cytokine, vascular endothelial growth factor (VEGF; GeneTex, Los Angeles, CA, USA), transforming growth factor-β (TGF-β; Thermo Fisher Scientific, Waltham, MA, USA), and both CD44 (FITC-conjugated; Biolegend, San Diego, CA, USA) and CD90 (APC/Cyanine7 conjugated; Biolegend) as the stem cell marker. Thereafter, fluorescent secondary antibody (AlexaFluor488-conjugated goat IgG; Thermo Fisher Scientific) and 4',6-diamidino-2-phenylindole (DAPI; Abcam, Cambridge, UK) were used. The Vectastain *Elite* ABC Rabbit kit (Vector Laboratories, Burlingame, CA, USA) was used as a marker of cell proliferation using a primary antibody against Ki67 (Abcam) as the cell-proliferation marker and transient receptor potential A1 (TRPA1; Funakoshi) as the receptor of pain. Sections treated without primary antibody were used as negative controls.

### 2.6. DPCs isolation and culture

DPCs were obtained from rat lower incisors and cultured as previously described [23]. DPCs at 3 to 5 passages were used in subsequent experiments at 80 % confluence and stimulated with 0–100 nM RvD2 and 1 μg/mL of lipopolysaccharide (LPS) from *Escherichia coli* (O111:B4, Sigma-Aldrich, St. Louis, MO, USA) for 24 and 48 h.

### 2.7. Cell-proliferation and cell-migration assays

The proliferation assay was performed using a tetrazolium salt-based assay (Cell Counting Kit-8; Dojindo Laboratories, Kumamoto, Japan) at 24 h. The migration assay was performed as previously described [29], with some modifications. After scraping with a 200-μL pipette tip to create a scratch on the confluent-grown cells, the cells were observed and photographed using a light microscope (ELWD 0.3/OD75; Nikon, Tokyo, Japan) at each time point. The relative width of each scratch was obtained by comparing the image at each time point to the one at baseline at time 0 as 100 %.

### 2.8. Real-time RT-PCR

Total RNA was extracted from cells using the RNeasy Mini Kit (Qiagen, Hilden, Germany), and the absorbance at 260 and 280 nm was measured for quantity and quality (A260/A280 = 1.8–2.2). Messenger RNA was reverse transcribed using the SuperScript VILO Master Mix (Thermo Fisher Scientific). Quantitative RT-PCR was conducted using the ABI 7300 system (Thermo Fisher Scientific) at 95 °C for 10 min, followed by 40 cycles at 95 °C for 15 s and 60 °C for 1 min in 96-well plates in a final volume of 20 μL containing SYBR green PCR master mix (Thermo Fisher Scientific) using specific primers (Supplemental Table). Data were analyzed using the comparative ( $-2^{\Delta\Delta C_t}$ ) method.

### 2.9. Enzyme-linked immunosorbent assay (ELISA)

VEGF and TGF-β in the culture supernatants were quantified by ELISA using the Rat VEGF-A ELISA Kit and TGF-β1 Rat Uncoated ELISA Kit (Thermo Fisher Scientific).

## 2.10. Flow cytometry

Cells subjected to 48-h culture were incubated with anti-CD16/CD32 (BioLegend, San Diego, CA, USA), followed by secondary antibodies: AlexaFluor647-labeled anti-CD73 and APC/Cy7-labeled anti-CD90 (BioLegend). Flow cytometry was performed using a MACSQuant-X (Miltenyi Biotec, Bergisch Gladbach, Germany). Data were analyzed using the FLOWJO software (BD Bioscience, Franklin Lakes, NJ, USA). Both CD73<sup>+</sup> and CD90-positive cells were defined as DPSCs [30,31].

## 2.11. Immune cell staining

DPCs were stained with primary antibodies against TRPA1 (Funakoshi), a pain receptor. Thereafter, fluorescent secondary antibodies (AlexaFluor488-conjugated goat IgG; Thermo Fisher Scientific) and DAPI were used.

## 2.12. Statistical analysis

All data are presented as the mean  $\pm$  standard deviation (SD). One-way analysis of variance (one-way ANOVA) was used to test for differences between three or more groups, and Tukey-Kramer test was used to test for multiple comparisons and Student's t-test was used to test the difference between the two groups, using Prism 8 for Windows (version 8.4.3: GraphPad Software, San Diego, CA, USA). A value of  $P < 0.05$  was considered statistically significant.

## 3. Results

### 1. Effect of RvD2 on reparative dentin bridge formation

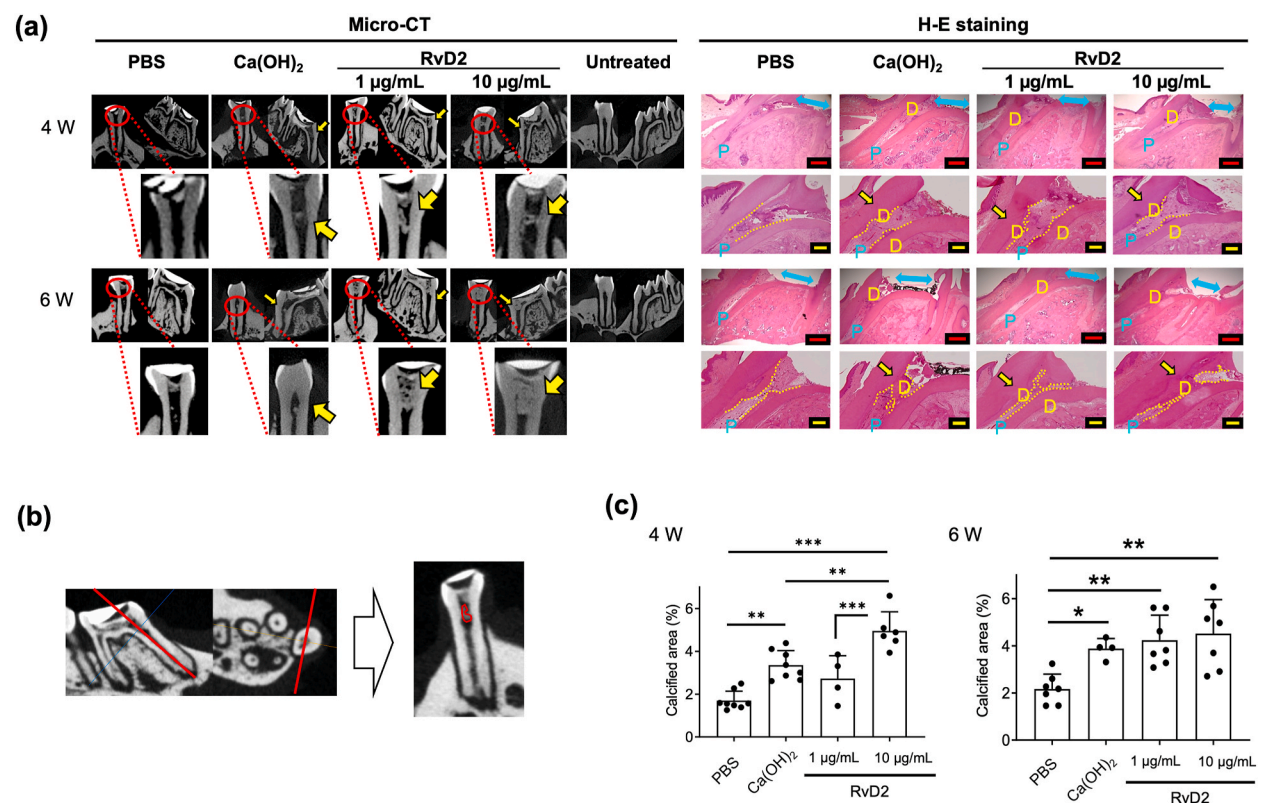
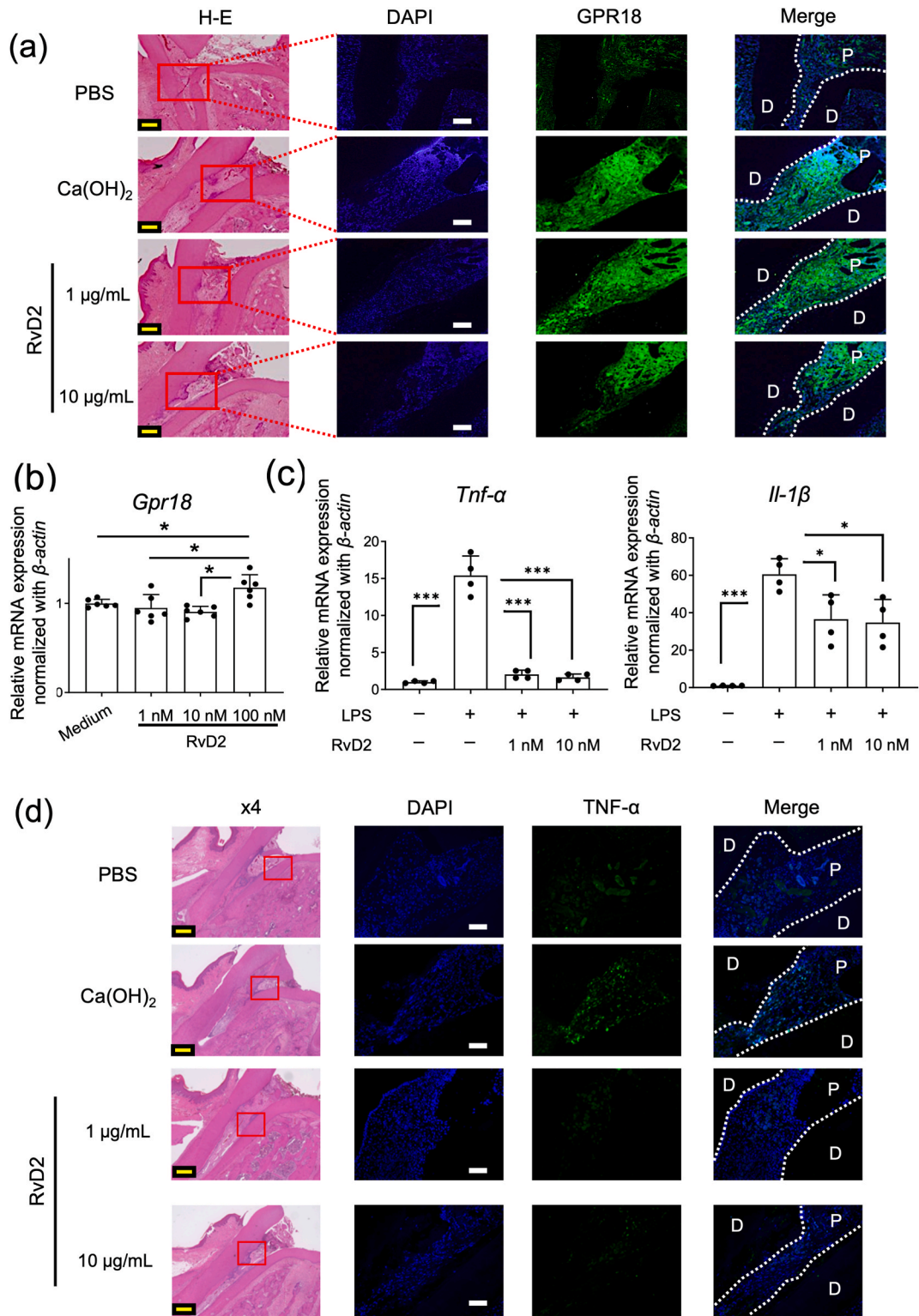


**Fig. 2.** Hard tissue formation after pulpotomy (a) Micro-CT and H-E staining images at 4 and 6 weeks after pulpotomy. Results from negative-control (PBS), positive-control (Ca(OH)<sub>2</sub>), and RvD2 application (1 μg/mL and 10 μg/mL; application of 3 μL) groups are shown. The yellow arrows indicate the hard tissue formed around the orifice of the root canal. In the RvD2 group and Ca(OH)<sub>2</sub> group, the areas were larger than those in the PBS group. Scale bars, red: 500 μm, yellow: 200 μm. (b) Area of the hard tissue for quantification. Representation of the rat pulpotomy experimental protocol. Data are shown as the means  $\pm$  SD (4-week samples include PBS: n = 8, Ca(OH)<sub>2</sub>: n = 8, RvD2 1 μg/mL: n = 4, and RvD2 10 μg/mL: n = 6; 6-week samples include PBS: n = 7, Ca(OH)<sub>2</sub>: n = 4, RvD2 1 μg/mL: n = 7, and RvD2 10 μg/mL: n = 7). \* $P < 0.05$ , \*\* $P < 0.01$ . One-way ANOVA was used to test for differences between three or more groups, and Tukey-Kramer test was used to test for multiple comparisons and Student's t-test was used to test the difference between the two groups. (For interpretation of the references to colour in this figure legend, the reader is referred to the Web version of this article.)





(caption on next page)

**Fig. 3.** Effects of RvD2 on the expression of its receptor and proinflammatory cytokines (a) Immunohistochemical analysis of GPR18 (green), a receptor for RvD2. D: dentine; P: pulp. Scale bars, yellow: 200  $\mu\text{m}$ , white: 100  $\mu\text{m}$ . Representatives of three independent *in vivo* samples are shown. (b) Relative gene expression of *Gpr18* in DPCs after 24-h culture. Data are shown as the means  $\pm$  SD (n = 6 wells/group). (c) Relative gene expression of *Il-1 $\beta$*  and *Tnf- $\alpha$*  in DPCs after 24-h culture. Data are shown as the means  $\pm$  SD (n = 4 wells/group). (d) Immunohistochemical analysis of TNF- $\alpha$  (green). D: dentine; P: pulp. Scale bars, yellow: 200  $\mu\text{m}$ , white: 100  $\mu\text{m}$ . Representatives of three independent *in vivo* samples are shown. \*P < 0.05. One-way ANOVA was used to test for differences between three or more groups, and Tukey-Kramer test was used to test for multiple comparisons and Student's t-test was used to test the difference between the two groups. (For interpretation of the references to colour in this figure legend, the reader is referred to the Web version of this article.)

According to radiological and histological analyses, reparative dentin was formed in both the RvD2 and Ca(OH)<sub>2</sub> groups compared with the rate at which it was formed in the PBS group at 4 and 6 weeks (Fig. 2a). The reparative dentin area (Fig. 2b) in both the RvD2 and Ca(OH)<sub>2</sub> groups was significantly higher than that in the PBS group at 4 and 6 weeks, although no statistical difference was observed between the RvD2 and Ca(OH)<sub>2</sub> groups (Fig. 2c).

## 2. Effect of RvD2 on GPR18 expression, inflammation, cell proliferation, and migration

The number of GPR18-positive cells *in vivo* (Fig. 3a) increased in both the RvD2 group and Ca(OH)<sub>2</sub> group compared with the number of GPR18-positive cells without RvD2 treatment. The mRNA expression levels in DPCs *in vitro* (Fig. 3b) increased following treatment with 100 nM RvD2 for 24 h. The mRNA expression levels of *Tnf- $\alpha$*  and *Il-1 $\beta$*  in DPCs *in vitro* with 1  $\mu\text{g}/\text{mL}$  of LPS stimulation for 24 h (Fig. 3c) decreased by RvD2 at 1 nM and 10 nM. The number of TNF- $\alpha$ -positive cells *in vivo* (Fig. 3d) decreased in the RvD2 group compared to the number of TNF- $\alpha$ -positive cells in the without RvD2 group and Ca(OH)<sub>2</sub> group.

RvD2 significantly promoted DPCs proliferation at 100 nM (Fig. 4a) *in vitro*. In addition, RvD2 enhanced the closure of the scratch area compared with its closure in the control at 24 and 48 h (Fig. 4BCE). Moreover, the number of Ki67-positive cells increased significantly in the RvD2 group, and the positive area increased in a dose-dependent manner *in vivo* (Fig. 4de).

## 3. Effect of RvD2 on induction of VEGF and TGF- $\beta$ from DPCs

The expression of *Vegf* and *Tgf- $\beta$*  mRNA at 24 h (Fig. 5a) and production of VEGF at 48 h (Fig. 5b) were promoted by RvD2 *in vitro*. VEGF-positive (Fig. 5c) and TGF- $\beta$ -positive areas (Fig. 5d) in both the RvD2 and Ca(OH)<sub>2</sub> groups were evident *in vivo* compared to the corresponding areas in the PBS group.

## 4. DPSCs induced by RvD2

*Nanog* mRNA expression increased in a dose-dependent manner following RvD2 addition *in vitro* (Fig. 6a). Furthermore, the number of CD44, CD73, and CD90 triple-positive cells increased upon RvD2 addition *in vitro* (Fig. 6b). In contrast, CD44 and CD90 double-positive cells were detected *in vivo* but were more clearly observed in the RvD2 group than in the PBS and Ca(OH)<sub>2</sub> groups (Fig. 6c).

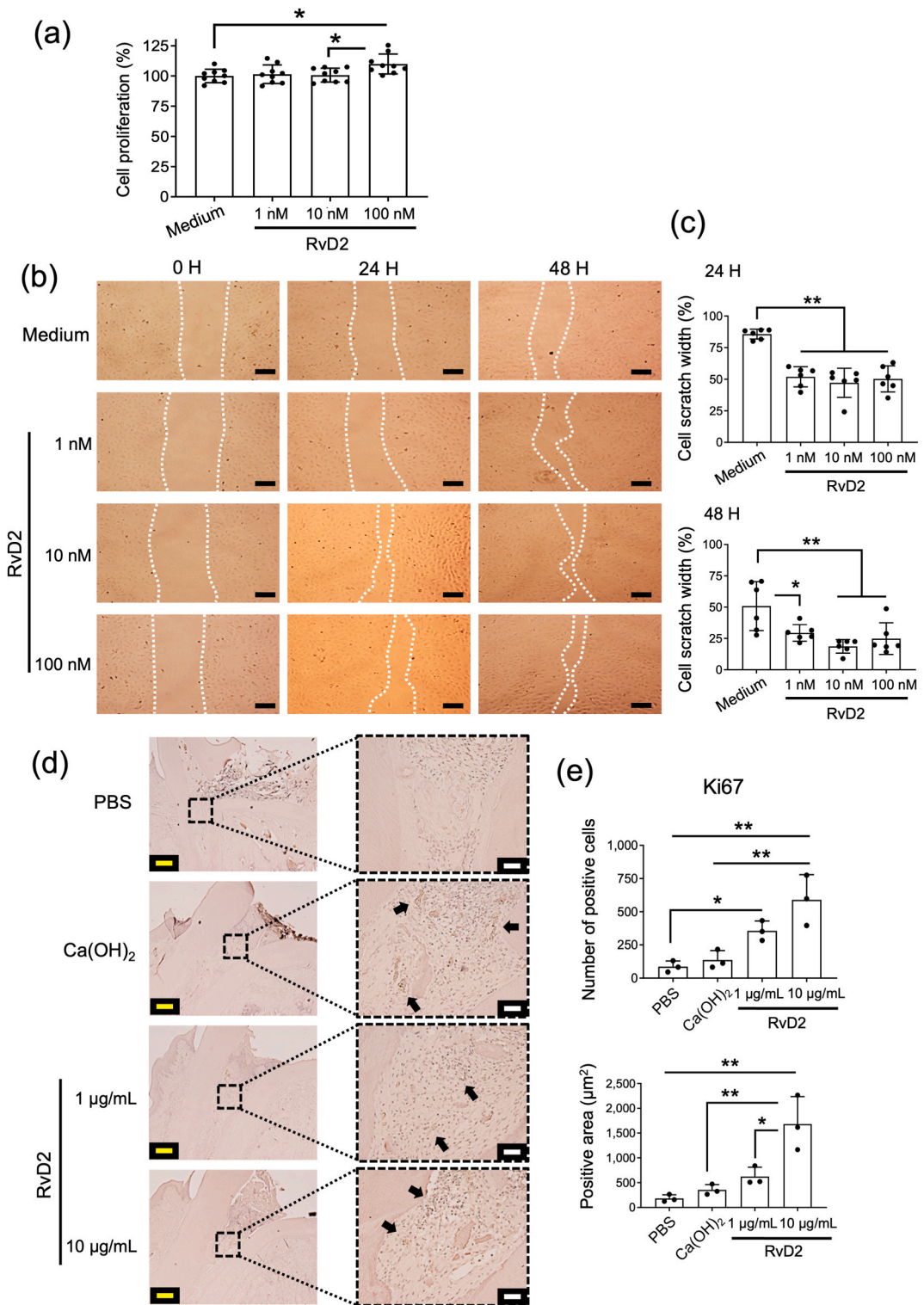
## 5. Decrease of TRPA1-positive cells in DPCs following RvD2 treatment

The number of TRPA1-positive cells *in vitro* (Fig. 7ab) decreased in the RvD2 group after LPS stimulation when compared to the number of them in the no-RvD2 group. Furthermore, the *Trpa1* mRNA expression level in DPCs *in vitro* increased following LPS stimulation but decreased by RvD2 addition (Fig. 7c). Moreover, the number of TRPA1-positive cells *in vivo* decreased prominently in the RvD2 group (Fig. 7de).

## 4. Discussion

In the present study, we analyzed the effects of RvD2 on the formation of calcified tissue at the orifice of the root canal following pulpotomy and performed immunohistochemical analyses using rat VPT and DPCs culture models. The results show that RvD2 induced the formation of reparative dentin and increased the number of DPSCs by promoting their proliferation.

First, we examined the ability of RvD2 to form reparative dentin using a pulpotomy model. Although calcium hydroxide has become a conventional pulp-capping reagent, it has been well known to cause generally the formation of reparative dentin in approximately four weeks [32,33]. Therefore, in the present study, the effect of RvD2 was analyzed at 4 and 6 weeks after pulpotomy, using calcium hydroxide as a positive control (Ca(OH)<sub>2</sub> group). We found that RvD2 induced the formation of reparative dentin superior to Ca(OH)<sub>2</sub> at four weeks and that reparative dentin formation at six weeks was almost same level. However, there were some low responders in RvD2-applied mice although well-calcified regions were detected by micro-CT analyses (Fig. 2). Furthermore, GPR18, a receptor for RvD2 [28], was expressed in the pulp tissues of both the RvD2 and Ca(OH)<sub>2</sub> groups. Therefore, RvD2 may induce the formation of reparative dentin by acting directly via GPR18 expressed on cells located in the amputated pulp tissue. We also inferred that RvD2 has an anti-inflammatory effect on DPCs (Fig. 3). Three  $\mu\text{L}$  of RvD2 solution (10  $\mu\text{g}/\text{mL}$  and 1  $\mu\text{g}/\text{mL}$ ) were absorbed in cotton pledget for this *in vivo* study, approximately equal to 30 ng and 10 ng of RvD2 (molecular weight: 376.5). These amounts were decided based on our previous *in vivo* study [28] and were fewer amounts than the RvE1 used for the direct pulp capping study [19] (50 ng; molecular weight: 350.4). Furthermore, it is well known that the concentration of RvD2 effective for



(caption on next page)

**Fig. 4.** Effects of RvD2 on the DPCs viability and migration (a) Viability of cultured DPCs in the presence of RvD2. Cell viability was compared to the medium-only group set at 100 %. (b, c) Migration of cultured DPCs in the presence of RvD2 after scratching the cell sheet. **b:** Representative images; **c:** quantification of scratch width. Scale bars: 200  $\mu\text{m}$ . (d, e) Ki67-positive cells in the dental pulp tissues ( $n = 3$  per group). **d:** Immunohistochemical analysis. Scale bars, yellow: 200  $\mu\text{m}$ , white: 100  $\mu\text{m}$ . **e:** Number of positive cells. \* $P < 0.05$ , \*\* $P < 0.01$ . One-way ANOVA was used to test for differences between three or more groups, and Tukey-Kramer test was used to test for multiple comparisons and Student's t-test was used to test the difference between the two groups. (For interpretation of the references to colour in this figure legend, the reader is referred to the Web version of this article.)

antiinflammation in the blood is 1 nM for leukocyte adherence and 10 nM for nitric oxide production [17], approximately equal to 376.5  $\mu\text{g}/\text{mL}$  and 3765  $\mu\text{g}/\text{mL}$  in weight/volume concentration. When the RvD2 concentration in animal and cell culture experiments are compared, the concentration in cell culture is 37.65 times more concentrated. In addition, the RvD2 solution applied to the pulpotomy area *in vivo*, RvD2 would be diluted with tissue fluid and blood. Thus, the optimum concentration of RvD2 *in vitro* may be no more than 10 nM.

To clarify the mechanisms by which RvD2 promotes the formation of reparative dentin, we examined the effects of RvD2 on DPCs *in vitro*. Cell proliferation and migration were promoted by RvD2 stimulation *in vitro* (Fig. 5a–c). Furthermore, when the cell-proliferative effect of RvD2 on the pulp tissue was examined *in vivo*, Ki67-positive cells, a marker of cell-proliferative potential, were observed in greater numbers in the RvD2 group than in the PBS and  $\text{Ca}(\text{OH})_2$  groups (Fig. 4). These results suggest that RvD2 may act on the pulp tissue and activate cell proliferation and migration. RvD2 reportedly promotes endothelial cell migration [34], consistent with the results of the present study. Hence, RvD2 may act on endothelial cells in DPCs to promote their proliferation.

To investigate the mechanism of cell proliferation, we analyzed the angiogenic cytokine VEGF and tissue-regenerative cytokine TGF- $\beta$  at the mRNA and protein levels *in vitro* according to their respective roles [35,36]. We observed that the mRNA expression levels of *Vegf* and *Tgf- $\beta$*  in DPCs were increased by RvD2 and only increased VEGF protein production. Furthermore, the localization of VEGF and TGF- $\beta$  was evident in the pulp tissue of the amputated region in the RvD2 group *in vivo* (Fig. 5). These results suggest that RvD2 induces angiogenesis by increasing the secretion of VEGF and TGF- $\beta$  in the pulp tissue. Consequently, the blood flow may increase in the pulp tissue of the amputated region. Moreover, TGF- $\beta$  may be secreted by various infiltrating hematogenous cells, leading to the proliferation of cells involved in the formation of reparative dentin, such as odontoblasts [37].

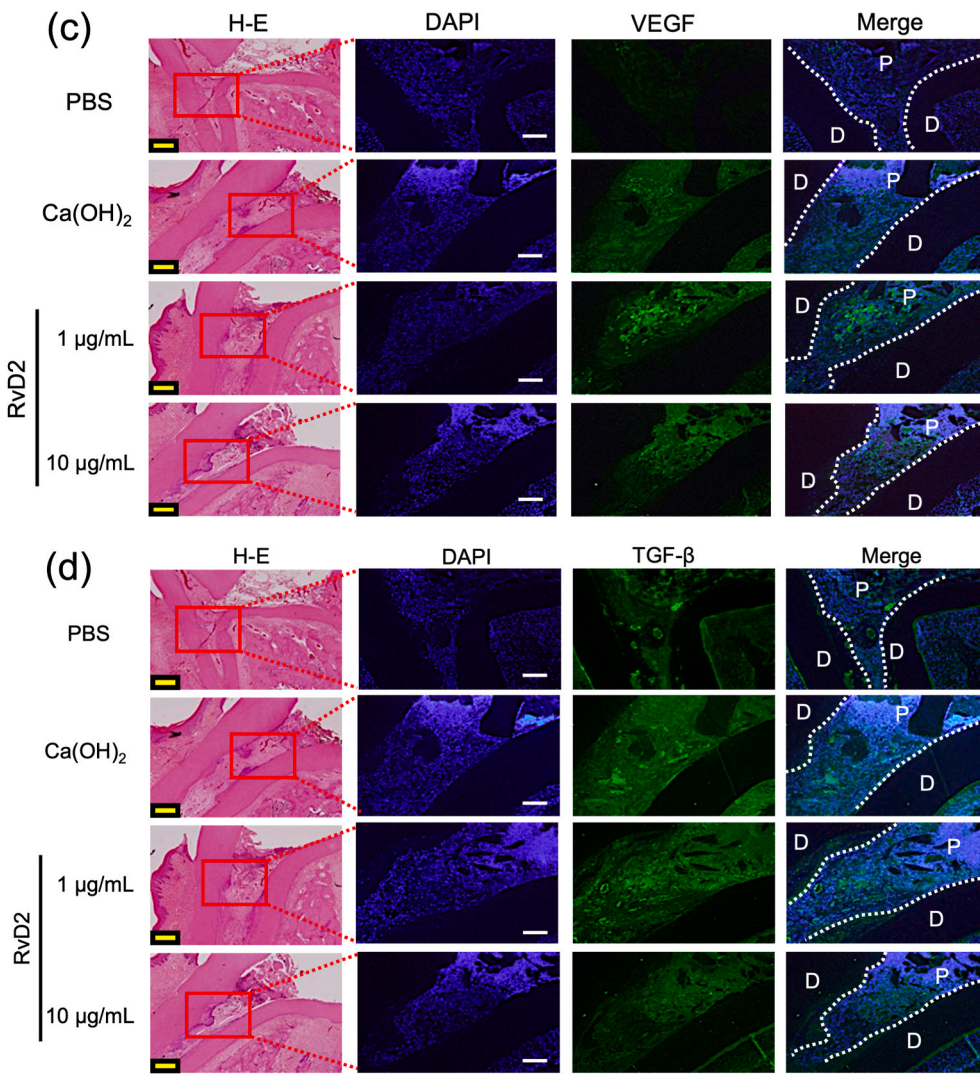
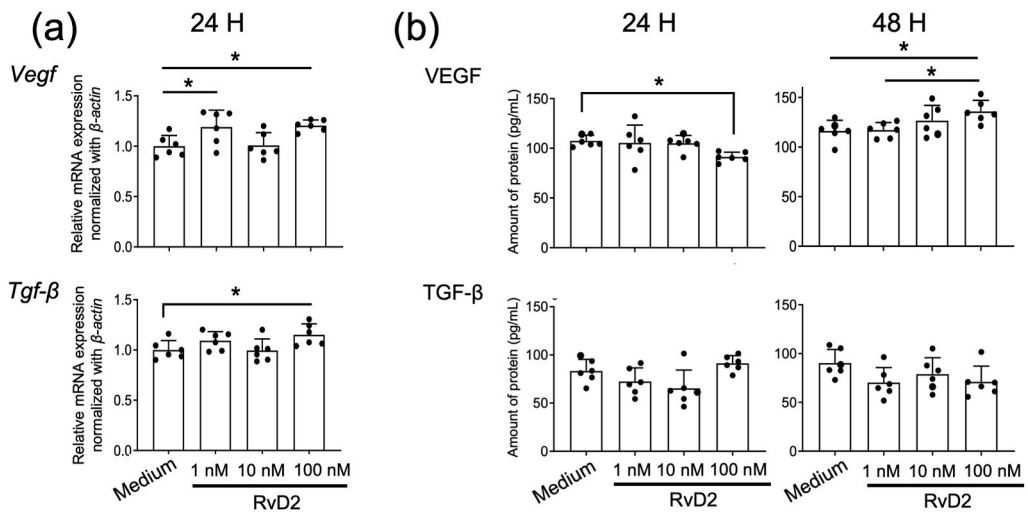
The effect of RvD2 on the induction of DPSCs, the most effective target of RvD2 for promoting the formation of reparative dentin, was examined *in vitro* because DPSCs differentiate into odontoblast-like cells and form reparative dentin [37,38]. In DPCs, RvD2 upregulated *Nanog* expression in a dose-dependent manner, which is gene-specific to pluripotent stem cells [39]. Additionally, the percentage of DPSCs was increased by RvD2 (Fig. 6), as revealed by flow cytometry analysis using the DPSC markers CD44, CD73, and CD90<sup>30,31</sup>. Resolvin E1 increases the number of DPSCs among DPCs [19], consistent with our results, suggesting that RvD2 may establish a favorable environment for reparative dentin formation by acting directly on DPSCs after pulpotomy. Although no significant difference was observed in the area of calcified tissue between RvD2 and  $\text{Ca}(\text{OH})_2$  (Fig. 2), RvD2 may be bio compatibly suitable for VPT, because it may promote neovascularization and DPSCs induction more than  $\text{Ca}(\text{OH})_2$ .

Finally, the effect of RvD2 on TRPA1, a pain receptor, which is a major issue in pulp capping [40], was investigated. In DPCs, the number of TRPA1-positive cells was increased by LPS stimulation and decreased by RvD2 treatment. In addition, *Trpa1* expression was decreased in DPCs following RvD2 treatment. Furthermore, *in vivo* experiments showed that the number of TRPA1-positive cells on the pulp tissue was reduced by RvD2 (Fig. 7). These results suggested that RvD2 suppresses pain while promoting hard tissue formation and that RvD2 has considerable potential for clinical applications. Related to this DPC culture model, there is a report describing the possible role of fibroblasts in mediating cold responses [41]. In addition, the odontoblasts may activate adjacent pulpal axons and thus contribute to dental pain and hypersensitivity [42], although there are still unknown relations for pain signaling between DPCs and odontoblasts. These mean that DPCs may contribute to the sensation of pulpal pain. Thus, reducing pain sensation in DPCs is important to vital pulp therapy when the RvD2 is applied as the therapeutic agent.

The present study has several limitations. Although we investigated whether RvD2 is involved in the differentiation of odontoblast-like cells, further investigations are warranted to determine the optimal dosage and frequency of application. RvD2 is metabolized *in vivo* within a few days [43]; therefore, a slow-release delivery system may be more efficacious. In addition, the recent standard for preserving dental pulp has become to use MTA [6,7], however, our purpose is to investigate the effects of RvD2 on the pulpal tissue after pulpotomy. Either MTA or calcium hydroxide paste may serve as the positive control for the calcification of pulpal tissue. In future studies, we plan similar experiments using larger animal models as MTA is a positive control. Further studies using larger animal models to clarify these issues will contribute to the development of RvD2 reagent as a novel VPT.

In the present study, RvD2 was applied directly to the pulpal surface at the pulpotomy site to induce reparative dentin formation. The possible mechanism may be related to the RvD2-induced increase in the secretion of cytokines related to tissue regeneration, such as VEGF and TGF- $\beta$ , in the pulp tissue by promoting cell proliferation. Furthermore, RvD2 may directly act on DPSCs and activate cell proliferation, thereby promoting reparative dentin formation. These results suggest that RvD2 can be used as a VPT and may exert reparative actions through a mechanism different from existing VPT reagents that do not induce inflammation [44]. RvD2 could also be used for next-generation VTP, comparable to stem cell transplantation-based therapies [45] and the application of a functional peptide derived from the protein S100 family [46]. Further validation experiments with RvD2 in rodent models of pulpitis induced by caries infection [47] and larger animals are required.





(caption on next page)



**Fig. 5.** Regenerative cytokines from cultured DPCs and pulp tissue after pulpotomy (a, b) **a:** Relative gene expression of *Vegf* and *Tgf- $\beta$*  in DPCs after 24-h culture. **b:** secretion of VEGF and TGF- $\beta$  by DPCs after 24- and 48-h culture. Data are shown as the means  $\pm$  SD (n = 6 wells/group). \*P < 0.05. One-way ANOVA was used to test for differences between three or more groups, and Tukey-Kramer test was used to test for multiple comparisons and Student's t-test was used to test the difference between the two groups. (c, d) Immunohistochemical analysis of VEGF (c) and TGF- $\beta$  (d) in *in vivo* dental pulp tissue. D: dentine; P: pulp. Scale bars, yellow: 200  $\mu$ m, white: 100  $\mu$ m. Representatives of three independent samples are shown. (For interpretation of the references to colour in this figure legend, the reader is referred to the Web version of this article.)

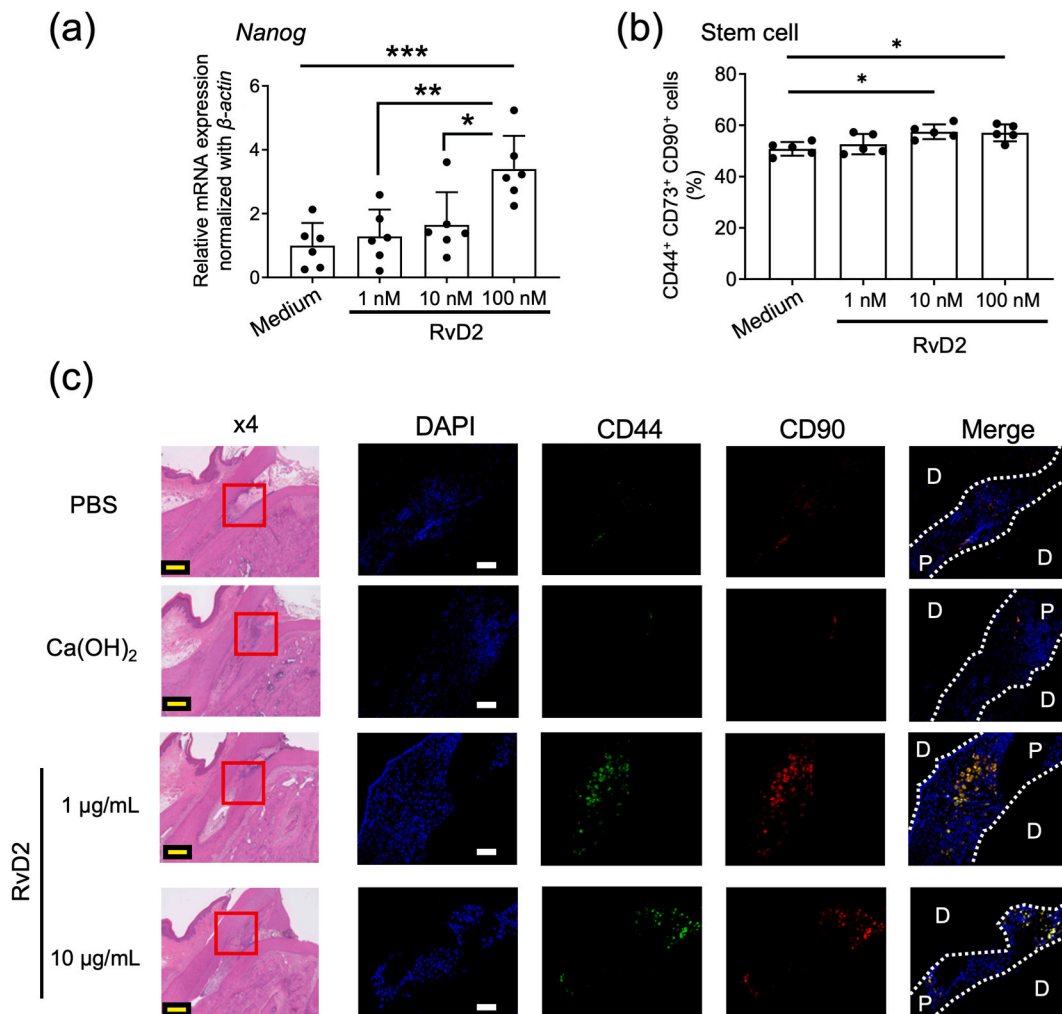
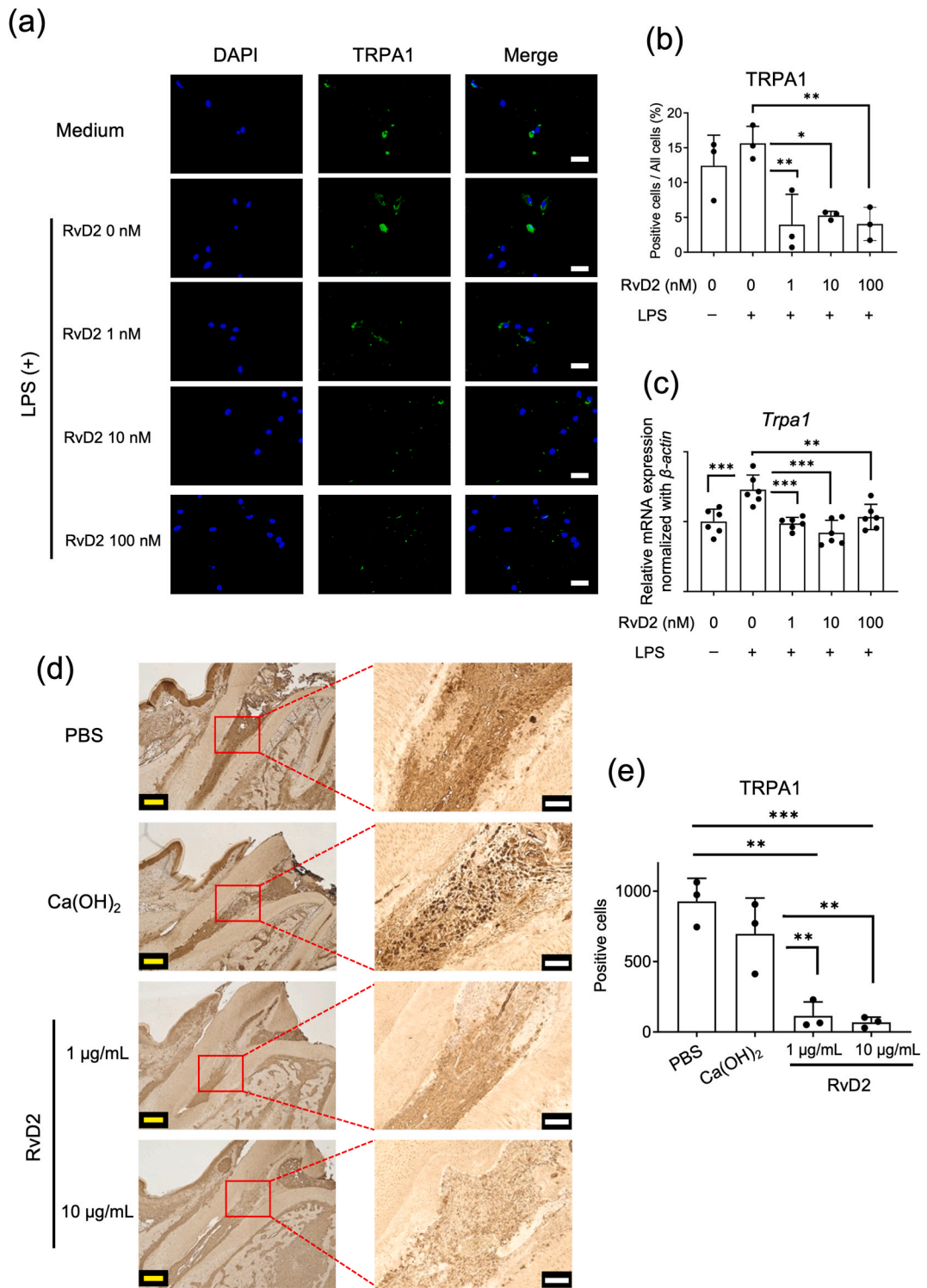


**Fig. 6.** Stem-like cells in cultured DPCs and pulp tissue after pulpotomy (a, b) **a:** Relative gene expression of *Nanog* in cultured DPCs. Data are shown as the means  $\pm$  SD (n = 6 wells/per group). **b:** Flow cytometric analysis of CD44<sup>+</sup> CD73<sup>+</sup> CD90<sup>+</sup> cells in cultured DPCs (passages 3–5) at confluence with 0–100 nM RvD2 for 2 days. The percentage of them in total cells in each well was measured. Data are shown as the means  $\pm$  SD (n = 5 wells/group). \*P < 0.05, \*\*P < 0.01, \*\*\*P < 0.001. One-way ANOVA was used to test for differences between three or more groups, and Tukey-Kramer test was used to test for multiple comparisons and Student's t-test was used to test the difference between the two groups. (c) Immunohistochemical analysis of CD44 (green) and CD90 (red) in dental pulp tissue. D: dentine; P: pulp. Scale bars, yellow: 200  $\mu$ m, white: 100  $\mu$ m. Representatives of three independent samples are shown. (For interpretation of the references to colour in this figure legend, the reader is referred to the Web version of this article.)

### Ethics statement

The Animal Care and Use Committee of Okayama University approved the research (OKU-2019575, OKU-2022375, OKU-2022679).



(caption on next page)

**Fig. 7.** Downregulated TRPA1 expression in cultured DPCs and pulp tissue after pulpotomy (a, b) **a:** Immunohistochemical analysis of TRPA1 (green) in DPCs (passage 3–5) at confluence with lipopolysaccharide (LPS; *E. coli*) and 0–100 nM RvD2 for 4 days. Scale bars, white: 50  $\mu$ m. **b:** Percentage of TRPA1-positive cells. Data are shown as the means  $\pm$  SD (n = 3 wells/group). (c) Relative expression of *Trpa1* in DPCs (passages 3–5) at confluence with the LPS and 0–100 nM RvD2 for 12 h. Data are shown as the means  $\pm$  SD (n = 6 wells/group). (d, e) **d:** Immunohistochemical analysis of TRPA1 in the dental pulp tissue beneath the pulpotomy (n = 3/group). Scale bars, yellow: 200  $\mu$ m, white: 100  $\mu$ m. **e:** Number of positive cells. \*P < 0.05, \*\*P < 0.01, \*\*\*P < 0.001. One-way ANOVA was used to test for differences between three or more groups, and Tukey-Kramer test was used to test for multiple comparisons and Student's t-test was used to test the difference between the two groups. (For interpretation of the references to colour in this figure legend, the reader is referred to the Web version of this article.)

## Data sharing statement

The data that support the findings of this study are available from the corresponding author upon reasonable request.

## Funding

The present study was supported, in part, by the JSPS KAKENHI (grant number 20K09938 for Z. A.).

## CRedit authorship contribution statement

**Mitsuhiro Yoneda:** Writing – original draft, Visualization, Methodology, Investigation, Data curation, Conceptualization. **Hide-taka Ideguchi:** Writing – original draft, Methodology, Investigation, Formal analysis. **Shin Nakamura:** Writing – review & editing, Formal analysis, Conceptualization. **Zulema Arias:** Writing – original draft, Validation, Supervision, Investigation, Funding acquisition, Conceptualization. **Mitsuaki Ono:** Writing – review & editing, Visualization, Investigation. **Kazuhiro Omori:** Writing – review & editing, Validation. **Tadashi Yamamoto:** Writing – review & editing, Validation, Supervision. **Shogo Takashiba:** Writing – review & editing, Validation, Supervision, Resources, Project administration, Conceptualization.

## Declaration of competing interest

The authors declare the following financial interests/personal relationships which may be considered as potential competing interests: Zulema Arias reports financial support was provided by Japan Society for the Promotion of Science. If there are other authors, they declare that they have no known competing financial interests or personal relationships that could have appeared to influence the work reported in this paper.

## Acknowledgments

The authors declare no conflicts of interest. We thank Drs. Kazu Hatanaka-Takeuchi, Masahiro Ito, Kentaro Okamoto, and Kazuya Tamura for their valuable suggestions. A supplemental appendix to this article is available online.

## Appendix A. Supplementary data

Supplementary data to this article can be found online at <https://doi.org/10.1016/j.heliyon.2024.e34206>.

## References

- [1] W. Zhang, P.C. Yelick, Vital pulp therapy—Current progress of dental pulp regeneration and revascularization, *International Journal of Dentistry* (2010) 856087, [10.1155%2F2010%2F856087](https://doi.org/10.1155%2F2010%2F856087).
- [2] I.L. Bjørnø, S. Simon, P.L. Tomson, H.F. Duncan, Management of deep caries and the exposed pulp, *Int. Endod. J.* 52 (7) (2019) 949–973, <https://doi.org/10.1111/iej.13128>.
- [3] G.T. Huang, Dental pulp and dentin tissue engineering and regeneration: advancement and challenge, *Frontiers in Bioscience (Elite Ed)* 3 (2) (2011) 788–800, <https://doi.org/10.2741/e286>.
- [4] P. Hörsted-Bindslev, V. Vilkinis, A. Sidlauskas, Direct capping of human pulps with a dentin bonding system or with calcium hydroxide cement, *Oral Surgery, Oral Medicine, Oral Pathology, and Oral Radiology* 96 (5) (2003) 591–600, [https://doi.org/10.1016/s1079-2104\(03\)00155-0](https://doi.org/10.1016/s1079-2104(03)00155-0).
- [5] L. Graham, P.R. Cooper, N. Cassidy, J.E. Nor, A.J. Sloan, A.J. Smith, The effect of calcium hydroxide on solubilisation of bio-active dentine matrix components, *Biomaterials* 27 (14) (2006) 2865–2873, <https://doi.org/10.1016/j.biomaterials.2005.12.020>.
- [6] A. Fasoulas, G. Keratiotis, L. Spinelis, N. Pandis, M.A.A. De Bruyne, R.J.G. De Moor, M.A. Meire, Comparative efficacy of materials used in patients undergoing pulpotomy or direct pulp capping in carious teeth: A systematic review and meta-analysis, *Clinical and Experimental Dental Research* 9 (6) (2023) 1129–1148, <https://doi.org/10.1002/cre2.767>.
- [7] E.J.N.L. Silva, K.P. Pinto, F.G. Belladonna, C.M.A. Ferreira, M.A. Versiani, G. De-Deus, Success rate of permanent teeth pulpotomy using bioactive materials: A systematic review and meta-analysis of randomized clinical trials, *Int. Endod. J.* 56 (9) (2023) 1024–1041, <https://doi.org/10.1111/iej.13939>.
- [8] H.F. Duncan, Present status and future directions-Vital pulp treatment and pulp preservation strategies, *Int. Endod. J.* 55 (Suppl 3) (2022) 497–511, <https://doi.org/10.1111/iej.13688>.
- [9] W.L.O. da Rosa, E. Piva, A.F. da Silva, Disclosing the physiology of pulp tissue for vital pulp therapy, *Int. Endod. J.* 51 (8) (2018) 829–846, <https://doi.org/10.1111/iej.12906>.

- [10] D. Ricucci, G. Bergenholtz, Histologic features of apical periodontitis in human biopsies, *Endod. Top.* 8 (1) (2004) 68–87, <https://doi.org/10.1111/j.1601-1546.2004.00097.x>.
- [11] A.R. Youssef, R. Emara, M.M. Taher, F.A. Al-Allaf, M. Almalki, M.A. Almasri, S.S. Siddiqui, Effects of mineral trioxide aggregate, calcium hydroxide, biodentine and Emdogain on osteogenesis, odontogenesis, angiogenesis and cell viability of dental pulp stem cells, *BMC Oral Health* 19 (1) (2019) 133, <https://doi.org/10.1186/s12903-019-0827-0>.
- [12] C.N. Serhan, S. Hong, K. Gronert, S.P. Colgan, P.R. Devchand, G. Mirick, R.-L. Moussignac, Resolvins: a family of bioactive products of omega-3 fatty acid transformation circuits initiated by aspirin treatment that counter proinflammation signals, *J. Exp. Med.* 196 (8) (2002) 1025–1037, <https://doi.org/10.1084/jem.20020760>.
- [13] C.N. Serhan, N. Chiang, T.E. Van Dyke, Resolving inflammation: dual anti-inflammatory and pro-resolution lipid mediators, *Nat. Rev. Immunol.* 8 (5) (2008) 349–361, <https://doi.org/10.1038/nri2294>.
- [14] U.N. Das, Essential fatty acids: biochemistry, physiology and pathology, *Biotechnol. J.* 1 (4) (2006) 420–439, <https://doi.org/10.1002/biot.200600012>.
- [15] H.S. Jónasdóttir, S. Nicolardi, W. Jonker, R. Derks, M. Palmblad, A. Ioan-Facsinay, R. Toes, Y.E. van der Burgt, A.M. Deelder, O.A. Mayboroda, et al., Detection and structural elucidation of esterified oxylipids in human synovial fluid by electrospray ionization-fourier transform ion-cyclotron mass spectrometry and liquid chromatography-ion trap-MS(3): detection of esterified hydroxylated docosapentaenoic acid containing phospholipids, *Anal. Chem.* 85 (12) (2013) 6003–6010, <https://doi.org/10.1021/ac400826z>.
- [16] J.F. Lima-Garcia, R.C. Dutra, K. da Silva, E.M. Motta, M.M. Campos, J.B. Calixto, The precursor of resolvin D series and aspirin-triggered resolvin D1 display anti-hyperalgesic properties in adjuvant-induced arthritis in rats, *Br. J. Pharmacol.* 164 (2) (2011) 278–293, <https://doi.org/10.1111/j.1476-5381.2011.01345.x>.
- [17] M. Spite, L.V. Norling, L. Summers, R. Yang, D. Cooper, N.A. Petasis, Resolvin D2 is a potent regulator of leukocytes and controls microbial sepsis, *Nature* 461 (7268) (2009) 1287–1291, <https://doi.org/10.1038/nature08541>.
- [18] H. Xu, J. Chen, J. Ge, K. Xia, S. Tao, Y. Su, Q. Zhang, Resolvin E1 Ameliorates pulpitis by suppressing dental pulp fibroblast activation in a chemerin receptor 23-dependent manner, *J. Endod.* 45 (9) (2019) 1126–1134.e1, <https://doi.org/10.1016/j.joen.2019.05.005>.
- [19] J. Chen, H. Xu, K. Xia, S. Cheng, Q. Zhang, Resolvin E1 accelerates pulp repair by regulating inflammation and stimulating dentin regeneration in dental pulp stem cells, *Stem Cell Res. Ther.* 12 (1) (2021) 75, <https://doi.org/10.1186/s13287-021-02141-y>.
- [20] X. Liu, C. Wang, L. Pang, Pan, Q. Zhang, Combination of resolvin E1 and lipoxin A4 promotes the resolution of pulpitis by inhibiting NF- $\kappa$ B activation through upregulating sirtuin 7 in dental pulp fibroblasts, *Cell Prolif.* 55 (5) (2022) e13227, <https://doi.org/10.1111/cpr.13227>.
- [21] Y.C. Wu, N. Yu, C.A. Rivas, N. Mehrnia, A. Kantarci, T.E. Van Dyke, RvE1 promotes Axin2<sup>+</sup> cell regeneration and reduces bacterial invasion, *J. Dent. Res.* 102 (13) (2023) 1478–1487, <https://doi.org/10.1177/00220345231197156>.
- [22] G. Mizraji, O. Heyman, T.E. Van Dyke, A. Wilensky, Resolvin D2 restrains Th1 immunity and prevents alveolar bone loss in murine periodontitis, *Front. Immunol.* 9 (2018) 785, <https://doi.org/10.3389/fimmu.2018.00785>.
- [23] Y.D. Siddiqui, K. Omori, T. Ito, K. Yamashiro, S. Nakamura, K. Okamoto, M. Ono, T. Yamamoto, T.E. Van Dyke, S. Takahiba, Resolvin D2 induces resolution of periapical inflammation and promotes healing of periapical lesions in rat periapical periodontitis, *Front. Immunol.* 10 (2019) 307, <https://doi.org/10.3389/fimmu.2019.00307>.
- [24] V. Nagendrababu, P.E. Murray, R. Ordinola-Zapata, O.A. Peters, I.N. Rôças, J.F. Siqueira Jr., E. Priya, J. Jayaraman, S.J. Pulikkotil, N. Suresh, et al., PRILE 2021 guidelines for reporting laboratory studies in Endodontology: explanation and elaboration, *Int. Endod. J.* 54 (9) (2021) 1491–1515, <https://doi.org/10.1111/iej.13565>.
- [25] V. Nagendrababu, A. Kishen, P.E. Murray, M.H. Nekoofar, J.A.P. Figueiredo, E. Priya, J. Jayaraman, S.J. Pulikkotil, J. Camilleri, R.M. Silva, et al., PRIASE 2021 guidelines for reporting animal studies in Endodontology: explanation and elaboration, *Int. Endod. J.* 54 (6) (2021) 848–857, <https://doi.org/10.1111/iej.13477>.
- [26] N. Percie du Sert, A. Ahluwalia, S. Alam, M.T. Avey, M. Baker, W.J. Browne, A. Clark, I.C. Cuthill, U. Dirnagl, M. Emerson, et al., Reporting animal research: Explanation and elaboration for the ARRIVE guidelines 2.0, *PLoS Biol.* 18 (7) (2020) e3000411, <https://doi.org/10.1371/journal.pbio.3000411>.
- [27] K. Ishimoto, S. Hayano, T. Yanagita, H. Kurosaka, N. Kawanabe, S. Itoh, M. Ono, T. Kuboki, H. Kamioka, T. Yamashiro, Topical application of lithium chloride on the pulp induces dentin regeneration, *PLoS One* 10 (3) (2015) e0121938, <https://doi.org/10.1371/journal.pone.0121938>.
- [28] N. Chiang, J. Dallil, R.A. Colas, C.N. Serhan, Identification of resolvin D2 receptor mediating resolution of infections and organ protection, *J. Exp. Med.* 212 (8) (2015) 1203–1217, <https://doi.org/10.1084/jem.20150225>.
- [29] C.C. Liang, A.Y. Park, J.L. Guan, *In vitro* scratch assay: a convenient and inexpensive method for analysis of cell migration *in vitro*, *Nat. Protoc.* 2 (2) (2007) 329–333, <https://doi.org/10.1038/nprot.2007.30>.
- [30] M. Dominici, K. Le Blanc, I. Mueller, I. Slaper-Cortenbach, F.C. Marini, D.S. Krause, R.J. Deans, A. Keating, D.J. Prockop, E.M. Horwitz, Minimal criteria for defining multipotent mesenchymal stromal cells. The International Society for Cellular Therapy position statement, *Cytotherapy* 8 (4) (2006) 315–317, <https://doi.org/10.1080/14653240600855905>.
- [31] W. Martens, E. Wolfs, T. Struys, C. Politis, A. Bronckaers, I. Lambrechts, Expression pattern of basal markers in human dental pulp stem cells and tissue, *Cells Tissues Organs* 196 (6) (2012) 490–500, <https://doi.org/10.1159/000338654>.
- [32] Q. Liu, Y. Ma, J. Wang, X. Zhu, Y. Yang, Y. Mei, Demineralized bone matrix used for direct pulp capping in rats, *PLoS One* 12 (3) (2017) e0172693, <https://doi.org/10.1371/journal.pone.0172693>.
- [33] M. Okamoto, Y. Takahashi, S. Komichi, P.R. Cooper, M. Hayashi, Dentinogenic effects of extracted dentin matrix components digested with matrix metalloproteinases, *Sci. Rep.* 8 (1) (2018) 10690, <https://doi.org/10.1038/s41598-018-29112-3>.
- [34] M.J. Zhang, B.E. Sansbury, J. Hellmann, J.F. Baker, L. Guo, C.M. Parmer, J.C. Prenner, D.J. Conklin, A. Bhatnagar, M.A. Creager, et al., Resolvin D2 enhances postischemic revascularization while resolving inflammation, *Circulation* 134 (9) (2016) 666–680, <https://doi.org/10.1161/circulationaha.116.021894>.
- [35] K. Janebodini, R. Chavanachat, A. Hays, R.M. Gil, Silencing VEGFR-2 hampers odontoblastic differentiation of dental pulp stem cells, *Front. Cell Dev. Biol.* 9 (2021) 665886, <https://doi.org/10.3389/fcell.2021.665886>.
- [36] T. Niwa, Y. Yamakoshi, H. Yamazaki, T. Karakida, R. Chiba, J.C.-C. Hu, T. Nagano, R. Yamamoto, J.P. Simmer, H.C. Margolis, et al., The dynamics of TGF- $\beta$  in dental pulp, odontoblasts and dentin, *Sci. Rep.* 8 (1) (2018) 4450, <https://doi.org/10.1038/s41598-018-22823-7>.
- [37] J. Krivanek, R.A. Soldatov, M.E. Kastriiti, T. Chontorotzea, A.N. Herdina, J. Petersen, B. Szarowska, M. Landova, V.K. Matejova, L.L. Holla, et al., Dental cell type atlas reveals stem and differentiated cell types in mouse and human teeth, *Nat. Commun.* 11 (1) (2020) 4816, <https://doi.org/10.1038/s41467-020-18512-7>.
- [38] K.J. Kang, C.J. Ryu, Y.J. Jang, Identification of dentinogenic cell-specific surface antigens in odontoblast-like cells derived from adult dental pulp, *Stem Cell Res. Ther.* 10 (1) (2019) 128, <https://doi.org/10.1186/s13287-019-1232-y>.
- [39] N. Kawashima, Characterisation of dental pulp stem cells: a new horizon for tissue regeneration? *Arch. Oral Biol.* 57 (1) (2012) 1439–1458, <https://doi.org/10.1016/j.archoralbio.2012.08.010>.
- [40] D. Hashem, F. Mannocci, S. Patel, A. Manoharan, J.E. Brown, T.F. Watson, A. Banerjee, Clinical and radiographic assessment of the efficacy of calcium silicate indirect pulp capping: a randomized controlled clinical trial, *J. Dent. Res.* 94 (4) (2015) 562–568, <https://doi.org/10.1177/0022034515571415>.
- [41] I.A. El Karim, G.J. Linden, T.M. Curtis, I. About, M.K. McGahon, C.R. Irwin, S.A. Killough, F.T. Lundy, Human dental pulp fibroblasts express the "cold-sensing" transient receptor potential channels TRPA1 and TRPM8, *J. Endod.* 37 (4) (2011) 473–478, <https://doi.org/10.1016/j.joen.2010.12.017>.
- [42] Y.S. Cho, C.H. Ryu, J.H. Won, H. Vang, S.B. Oh, J.Y. Ro, Y.C. Bae, Rat odontoblasts may use glutamate to signal dentin injury, *Neuroscience* 335 (2016) 54–63, <https://doi.org/10.1016/j.neuroscience.2016.08.029>.
- [43] N. Giannakis, B.E. Sansbury, A. Patsalos, T.T. Hays, C.O. Riley, X. Han, M. Spite, L. Nagy, Dynamic changes to lipid mediators support transitions among macrophage subtypes during muscle regeneration, *Nat. Immunol.* 20 (5) (2019) 626–636, <https://doi.org/10.1038/s41590-019-0401-6>.
- [44] T.J. Hilton, Keys to clinical success with pulp capping: a review of the literature, *Operat. Dent.* 34 (5) (2009) 615–625, <https://doi.org/10.2341/09-132-0>.

- [45] M.A. Sabeti, M. Saqib Ihsan, D. Adami, S.-N. Hassani, S. Moushekhian, R. Shafieian, H. Salari Sedigh, J. Ghoddusi, Cell-based regenerative endodontics for the treatment of irreversible pulpitis: An in vivo investigation, *J. Endod.* 50 (3) (2024) 344–350, <https://doi.org/10.1016/j.joen.2023.11.014>.
- [46] M. Watanabe, M. Okamoto, S. Komichi, H. Huang, S. Matsumoto, K. Moriyama, J. Ohshima, S. Abe, M. Morita, M. Ali, et al., Novel functional peptide for next-generation vital pulp therapy, *J. Dent. Res.* 102 (3) (2023) 322–330, <https://doi.org/10.1177/00220345221135766>.
- [47] H. Huang, M. Okamoto, M. Watanabe, S. Matsumoto, K. Moriyama, S. Komichi, M. Ali, S. Matayoshi, R. Nomura, K. Nakano, et al., Development of rat caries-induced pulpitis model for vital pulp therapy, *J. Dent. Res.* 102 (5) (2023) 574–582, <https://doi.org/10.1177/00220345221150383>.